MMLDT CSET 2021

Data-driven prognostic model for temperature field in additive manufacturing based on the high-fidelity thermal-fluid flow simulation

Fan CHEN

(4th year PHD student)

Email: e0348805@u.nus.edu

Supervisor: Prof. Wentao YAN

Email: mpeyanw@nus.edu.sg

NUS National University of Singapore | Department of Mechanical Engineering, Faculty of Engineering

Problem

Powder bed fusion (PBF)

Thermal-fluid flow simulation

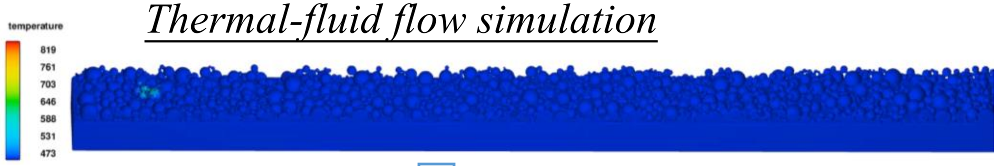

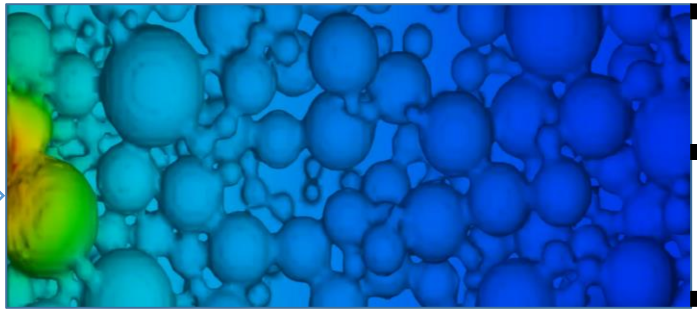

Phase transfer:
- Melting and solidification
- Evaporation, etc.

Heat transfer:
- Heat absorption
- Heat conduction, radiation, etc.

Fluid dynamics:
- Marangoni convection
- Capillarity, etc.

Grain growth

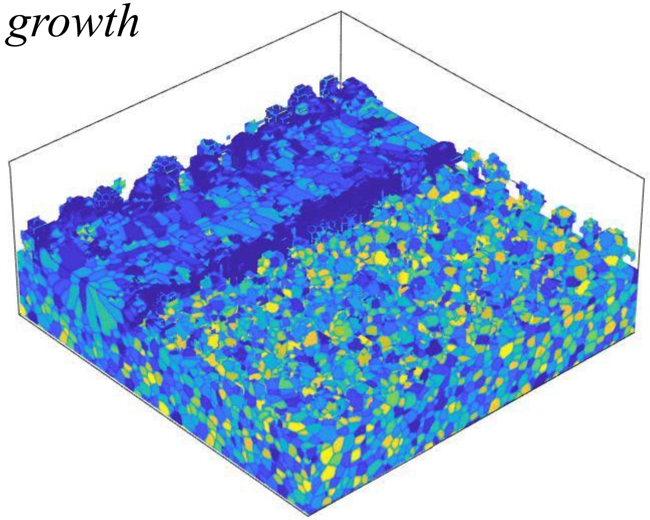

Thermal stress

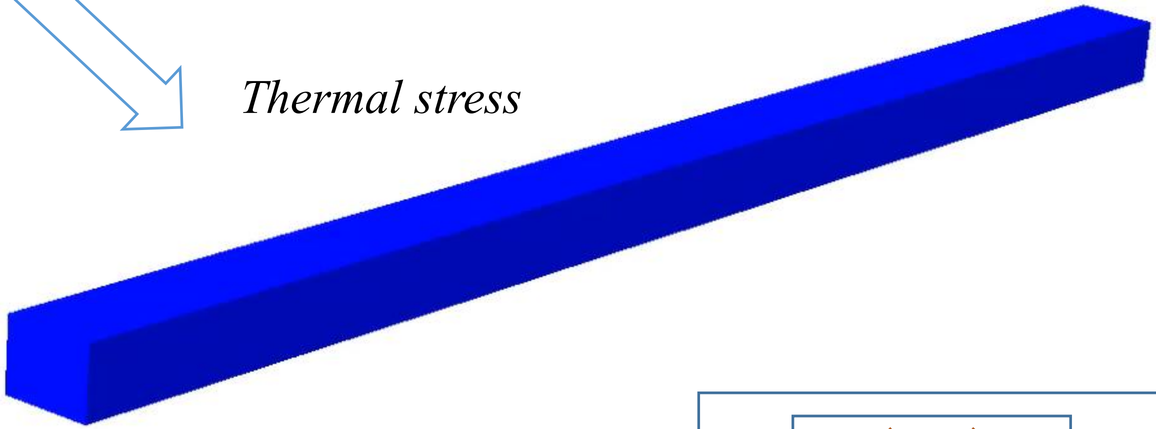

- High computational cost of the thermal-fluid flow simulation;
- Complex pre-processing of the temperature profiles;
- High computational cost of the temperature loading.

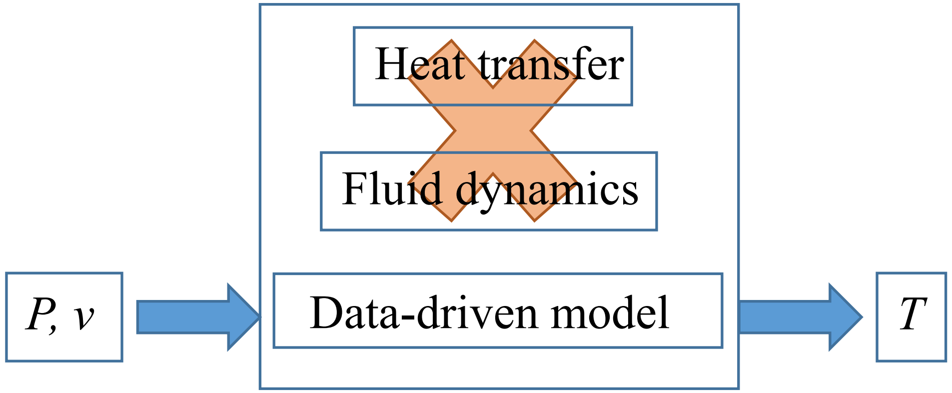

Overall framework

Data preparation

Isothermal points of $T(n_T) \pm \Delta T$

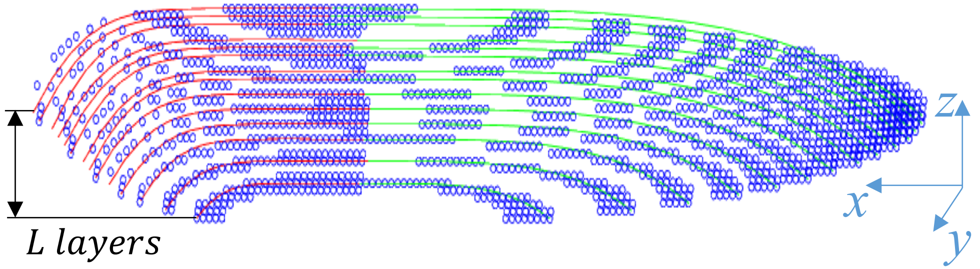

Curve fitting & parameterization

Isotherms

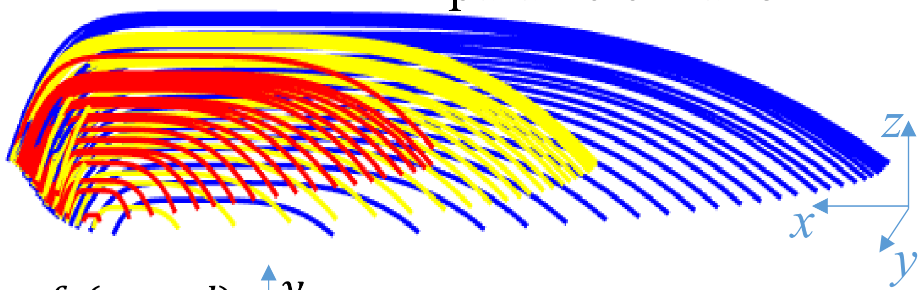

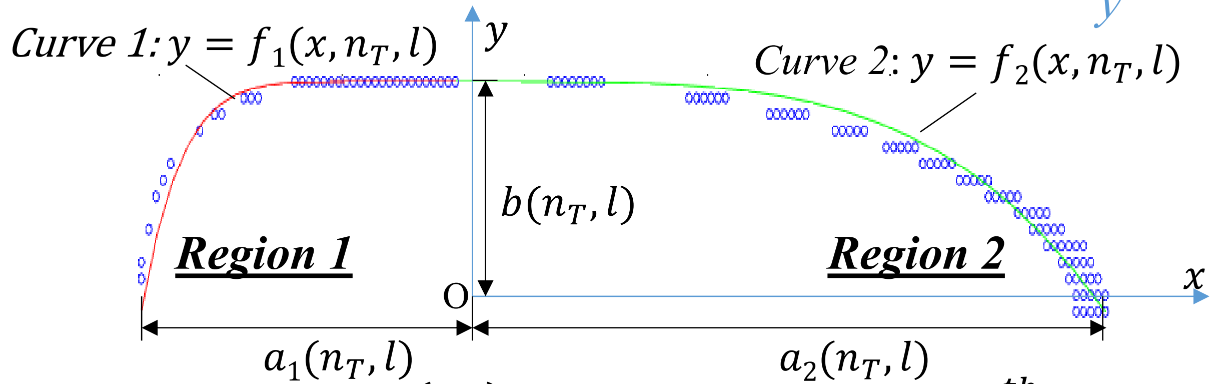

Curve-fitting of the $T(n_T)$ isothermal points at the l^{th} layer

Training data: thermal-fluid flow simulation

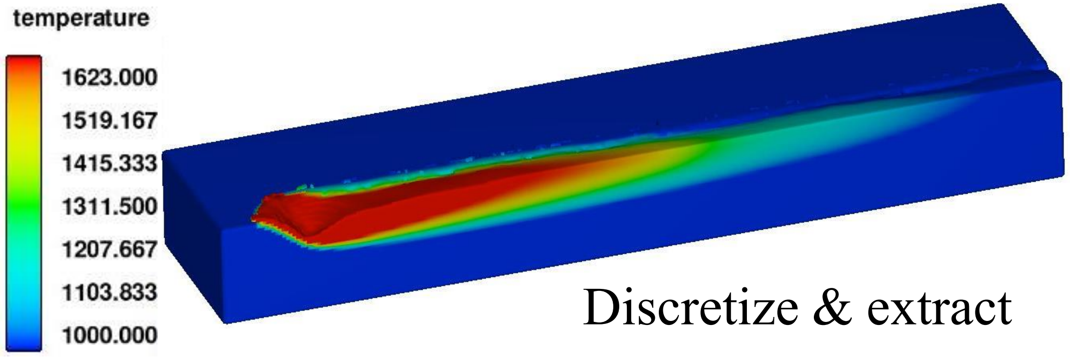

Discretize & extract

Regression/machine learning algorithms

INPUT: manufacturing parameters

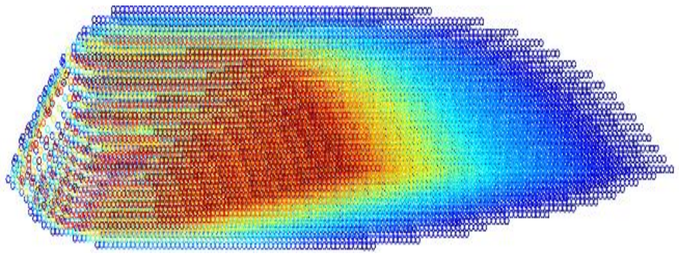

OUTPUT: isotherm dimensions to reconstruct temperature field

EVALUATION: Thermal stress model/ Grain growth model

Model construction

Temperature field parameterization

Training data: thermal-fluid flow simulation

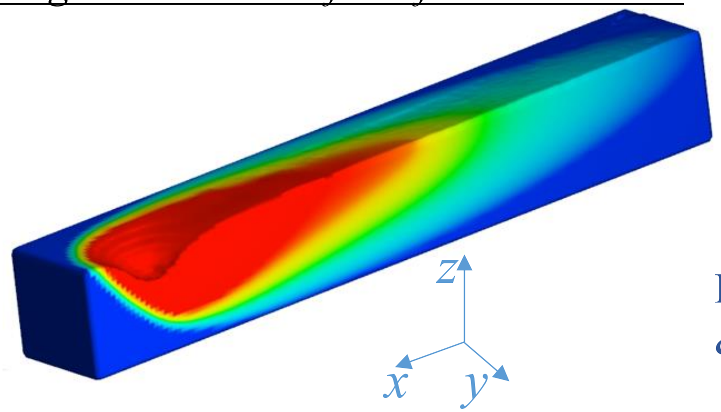

Discretize & extract

Isothermal points of $(T(n_T) \pm \Delta T)\ K$

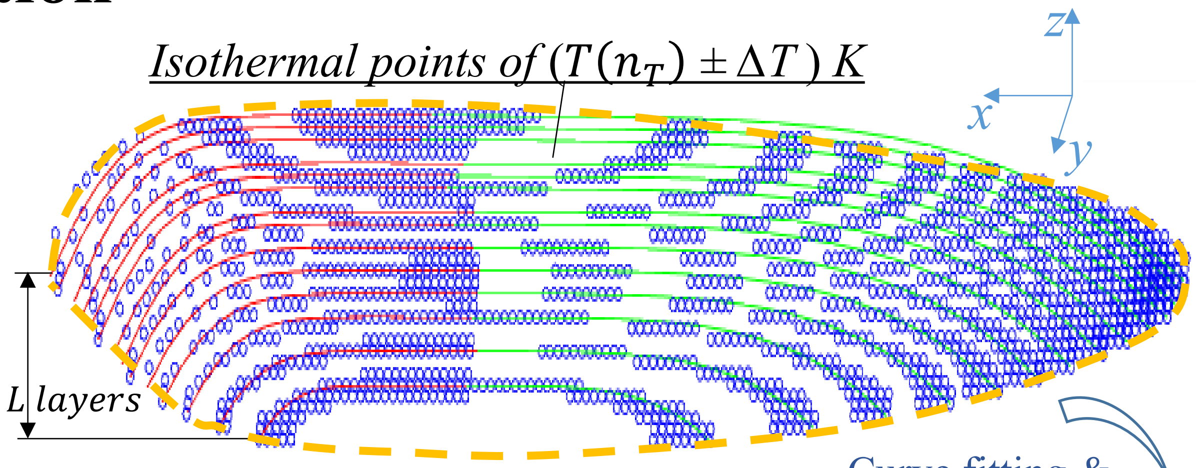

Curve fitting & parameterization

Isotherms

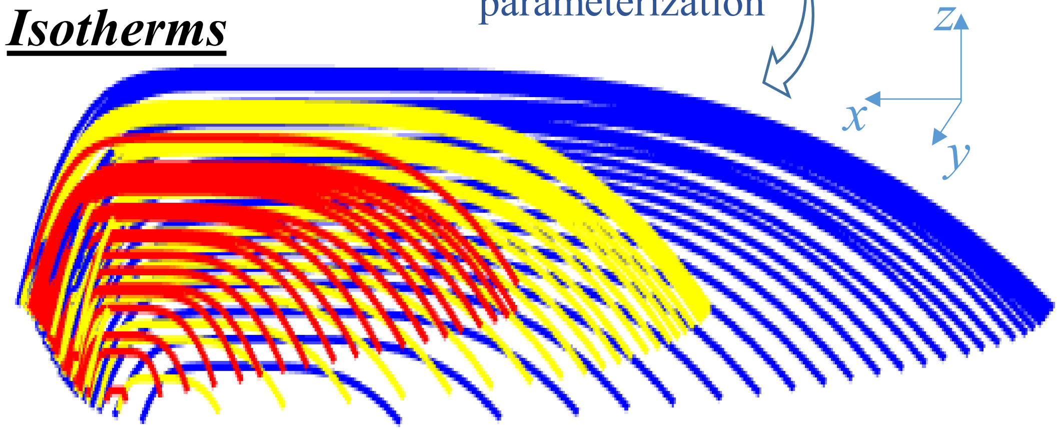

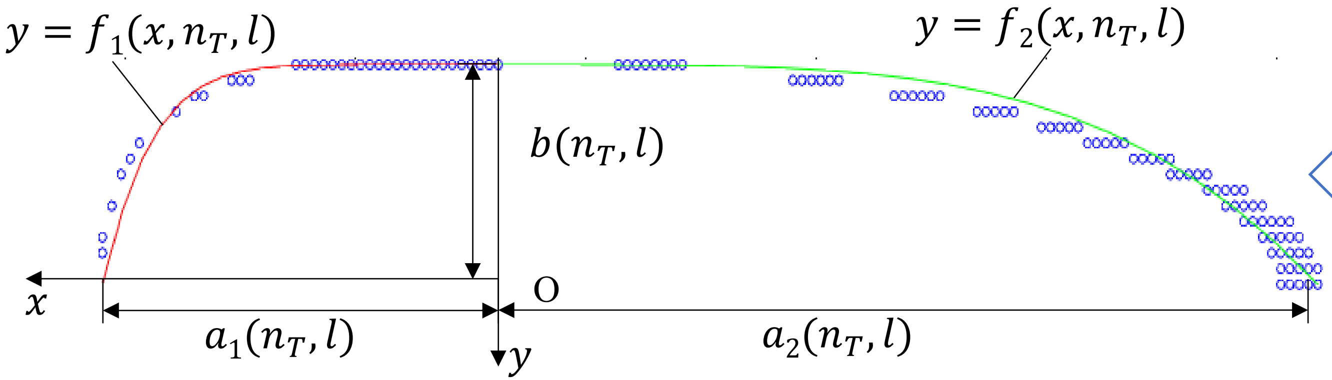

Curve-fitting of the $T(n_T)$ isothermal points at the l^{th} layer

Output variables: a_1, a_2, b

Model construction

Accuracy of the isotherms extraction (Inconel 625)

The grain evolution and thermal stress are essentially determined by the temperature field **at and around the molten pool boundary (1000~1560 K)**.

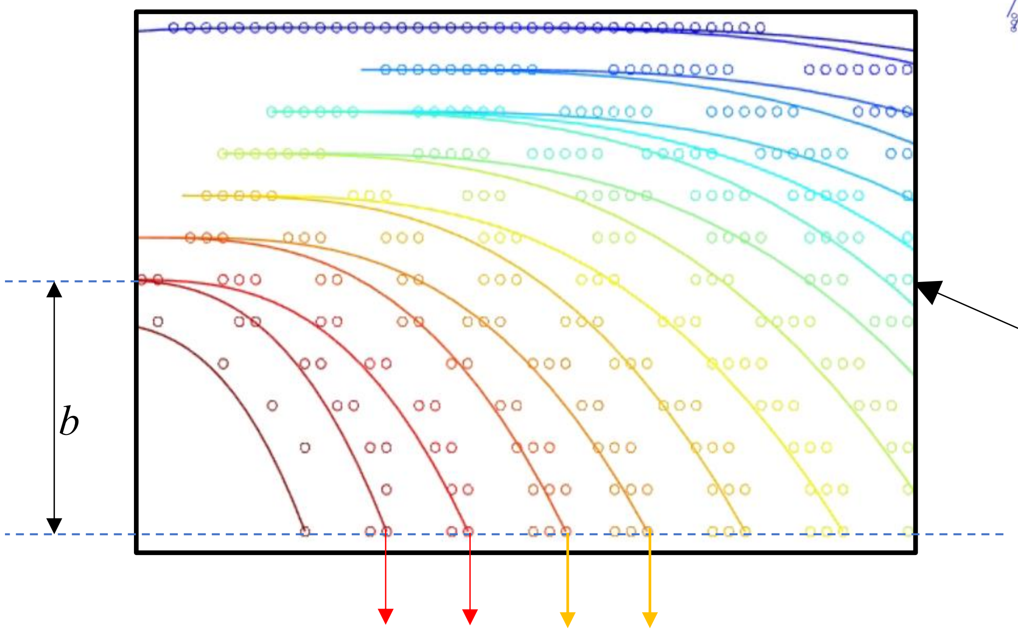

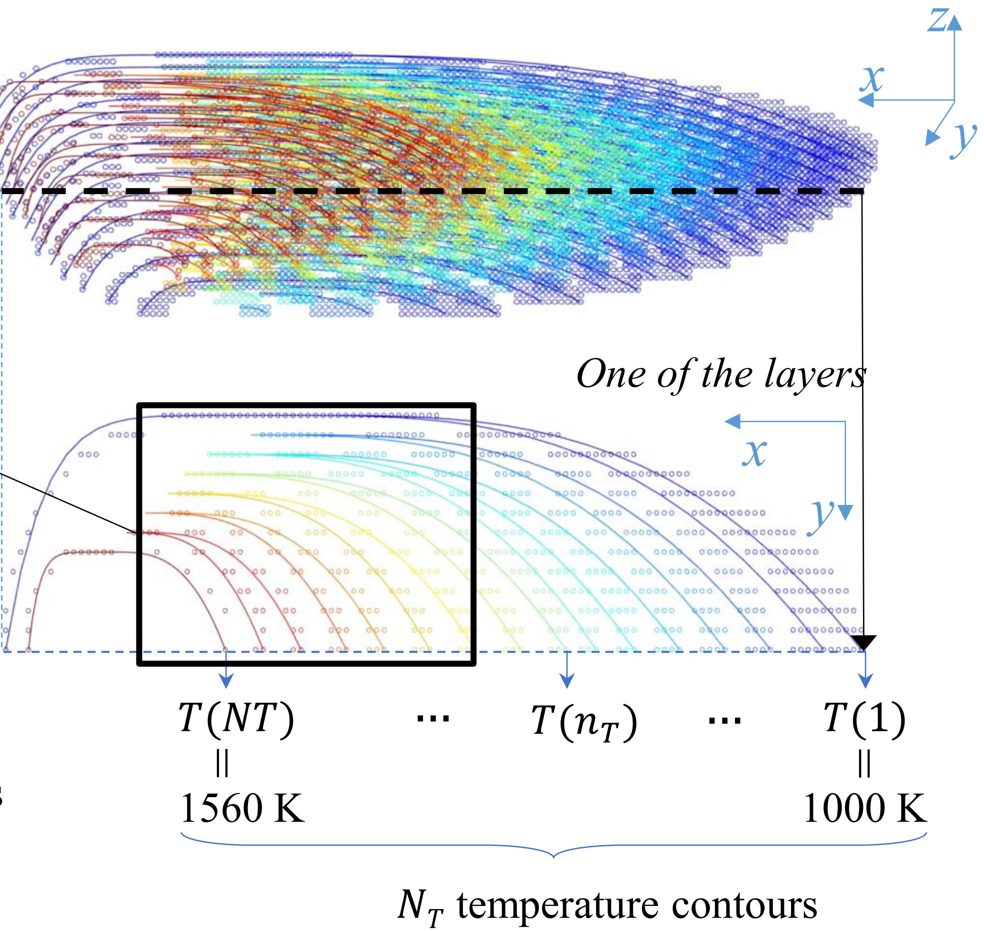

<u>**Half-width *b* captured inaccurately:**</u> Different contours share the same half-width *b* due to the limited mesh size.

Two main factors:

1. Contour numbers
2. Mesh size of the simulation

Below 1000 K, the solid-state phase transformations barely occur and the residual stresses do not change much.

Temperature field parameterization

Output variable: L

Curve shape and temperature gradient in two regions are quite different.

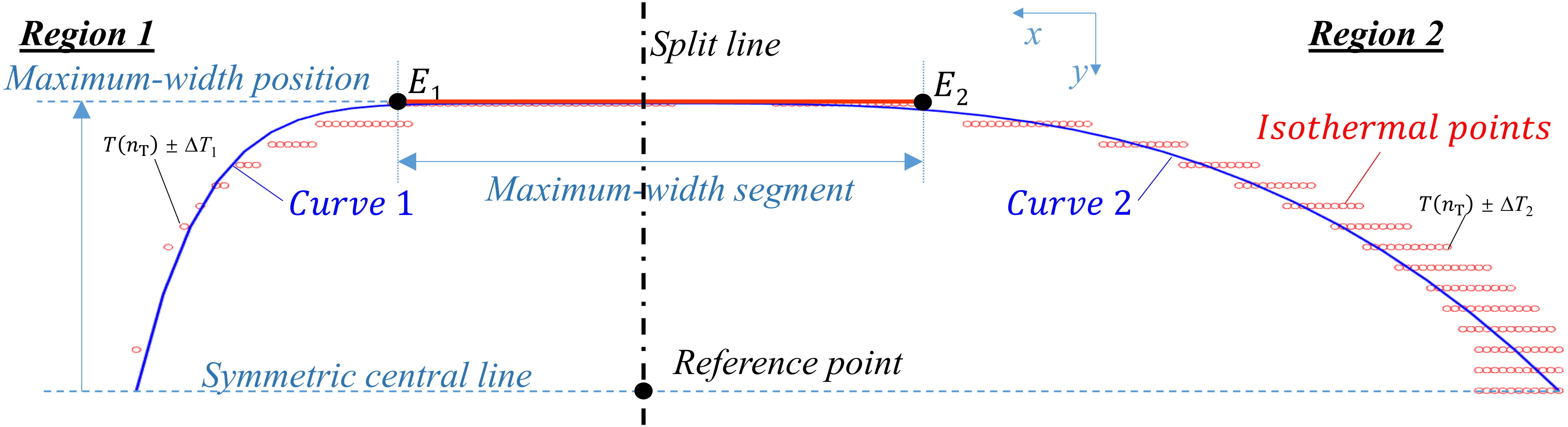

Fitting of the isothermal points of $(T(n_T) \pm \Delta T)$ K

Model construction

Fitting of the reference lines

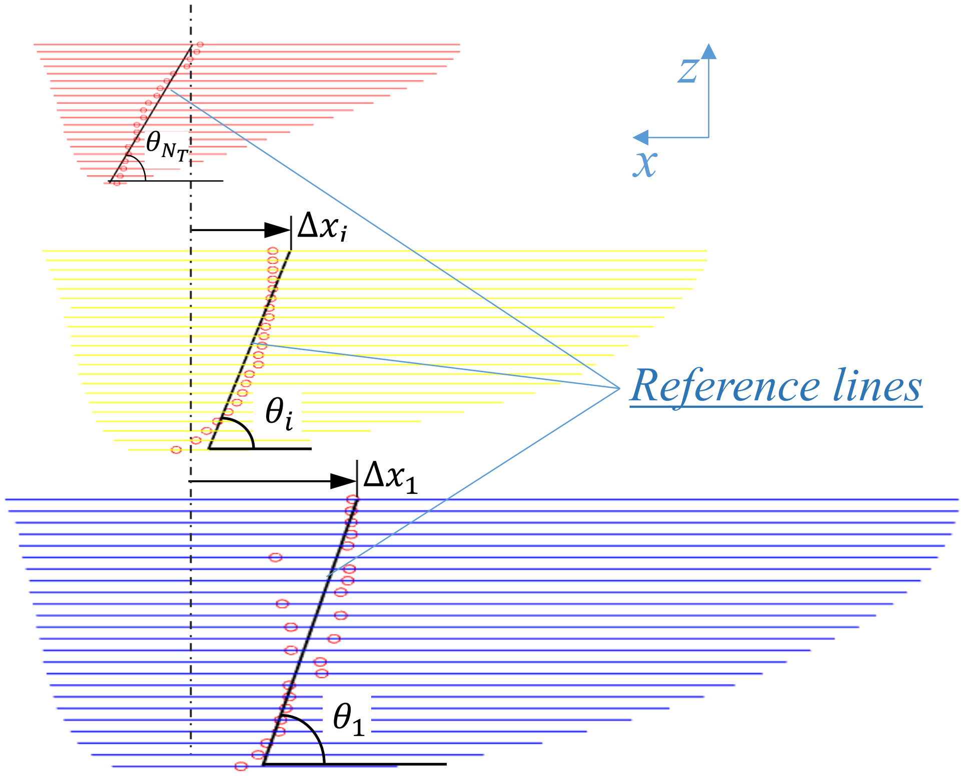

Output variables: $\Delta x, \theta, L$

Longitudinal symmetric plane

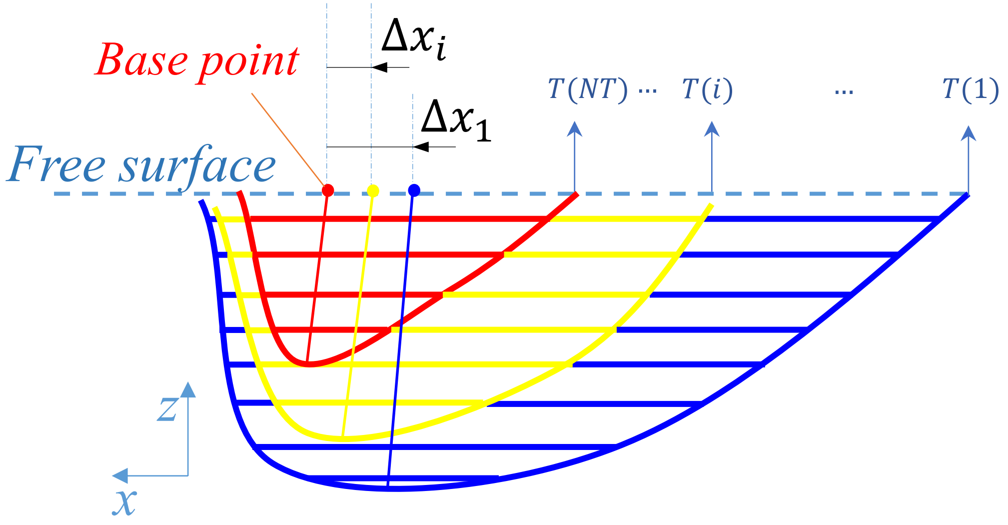

3D view

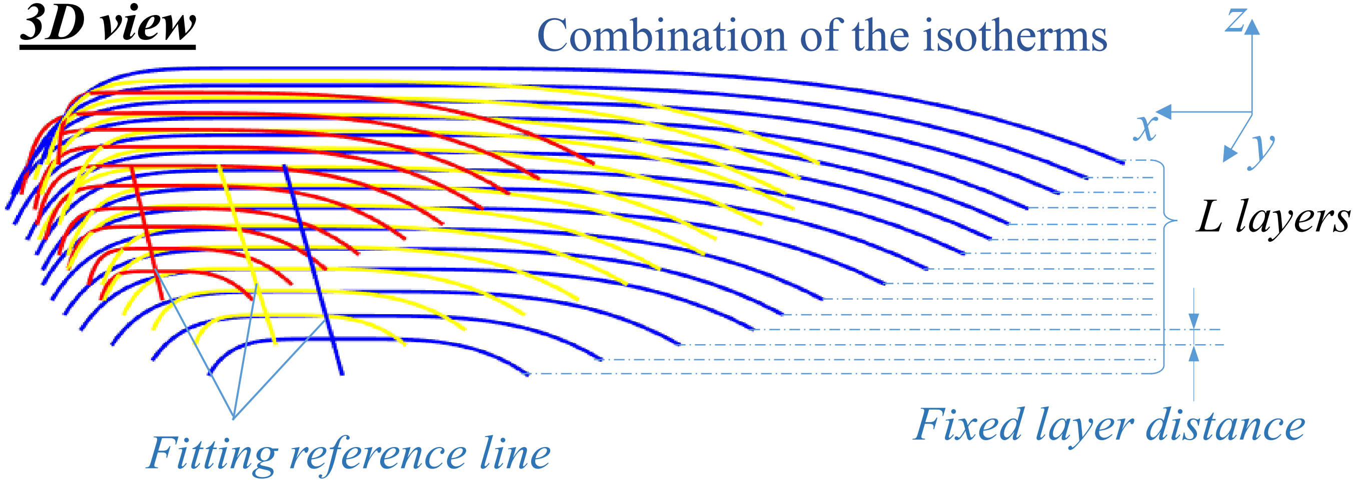

Model construction (Inconel 625)

MMLDT CSET 2021

NUS National University of Singapore

Input: ***manufacturing parameters for the thermal-fluid flow simulation samples*** $[V, P]$

(Samples. No.1 ~42, Each case costs about 100 CPU hours)

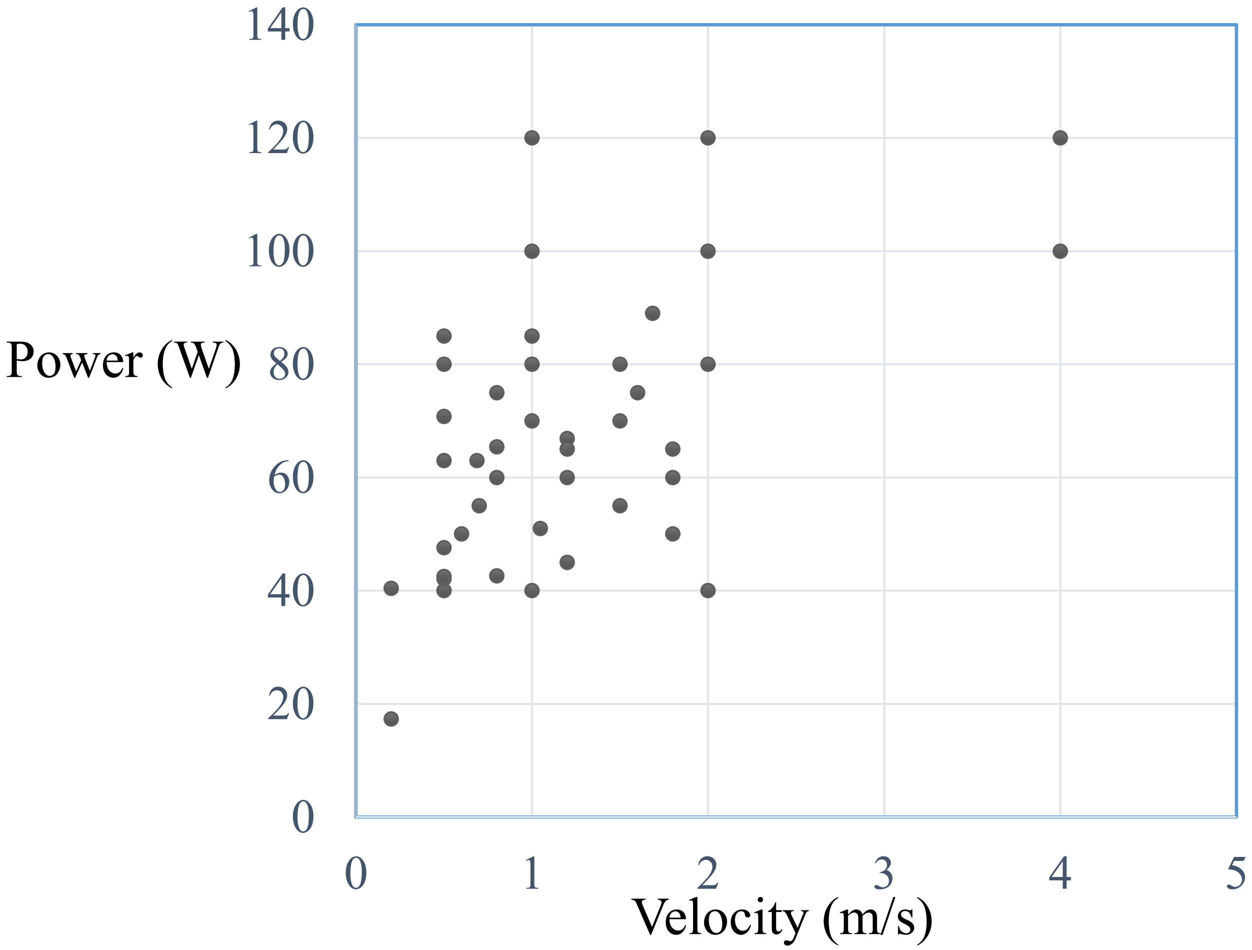

Data-driven algorithms

Output: ***the geometry features of the isotherms*** $[a_1, a_2, b, L, \theta, \Delta x, T_{peak}]$

Model construction

Data-driven algorithms

Gaussian process regression (GPR)

$$\boldsymbol{f} = [\boldsymbol{f}(\boldsymbol{x}_1), f(\boldsymbol{x}_2), \ldots, f(\boldsymbol{x}_n)]^\top$$

$$P_0(\boldsymbol{f} \mid \boldsymbol{X}) \sim \mathcal{N}(\boldsymbol{f} \mid 0, \boldsymbol{K}(\boldsymbol{X}, \boldsymbol{X}))$$

$$\begin{bmatrix} \boldsymbol{Y} \\ \boldsymbol{f}_* \end{bmatrix} \sim \mathcal{N}\left(\boldsymbol{0}, \begin{bmatrix} \boldsymbol{K}(\boldsymbol{X}, \boldsymbol{X}) + \sigma_n^2 \boldsymbol{I} & \boldsymbol{K}(\boldsymbol{X}, \boldsymbol{X}_*) \\ \boldsymbol{K}(\boldsymbol{X}_*, \boldsymbol{X}) & \boldsymbol{K}(\boldsymbol{X}_*, \boldsymbol{X}_*) \end{bmatrix}\right)$$

$$\begin{cases} P_0(\boldsymbol{f}_* \mid \boldsymbol{X}_*) \sim \mathcal{N}(\mu_*, \sigma_*^2) \\ \mu_* = \boldsymbol{K}(\boldsymbol{X}_*, \boldsymbol{X}) \left[\boldsymbol{K}(\boldsymbol{X}, \boldsymbol{X}) + \sigma_n^2 \boldsymbol{I}\right]^{-1} \boldsymbol{f} \\ \sigma_*^2 = \boldsymbol{K}(\boldsymbol{X}_*, \boldsymbol{X}_*) - \boldsymbol{K}(\boldsymbol{X}_*, \boldsymbol{X}) \left[\boldsymbol{K}(\boldsymbol{X}, \boldsymbol{X}) + \sigma_n^2 \boldsymbol{I}\right]^{-1} \boldsymbol{K}(\boldsymbol{X}, \boldsymbol{X}_*) \end{cases}$$

Quadratic regression (QR)

$$\eta = \beta_0 + \sum_{j=1}^{k} \beta_j x_j + \sum_{j=1}^{k} \beta_{jj} x_j^2 + \sum_{i=1, j=2}^{k} \beta_{ij} x_i x_j$$

Two main factors:

1. High accuracy
2. Fast predicting speed

Feedforward neuronal network

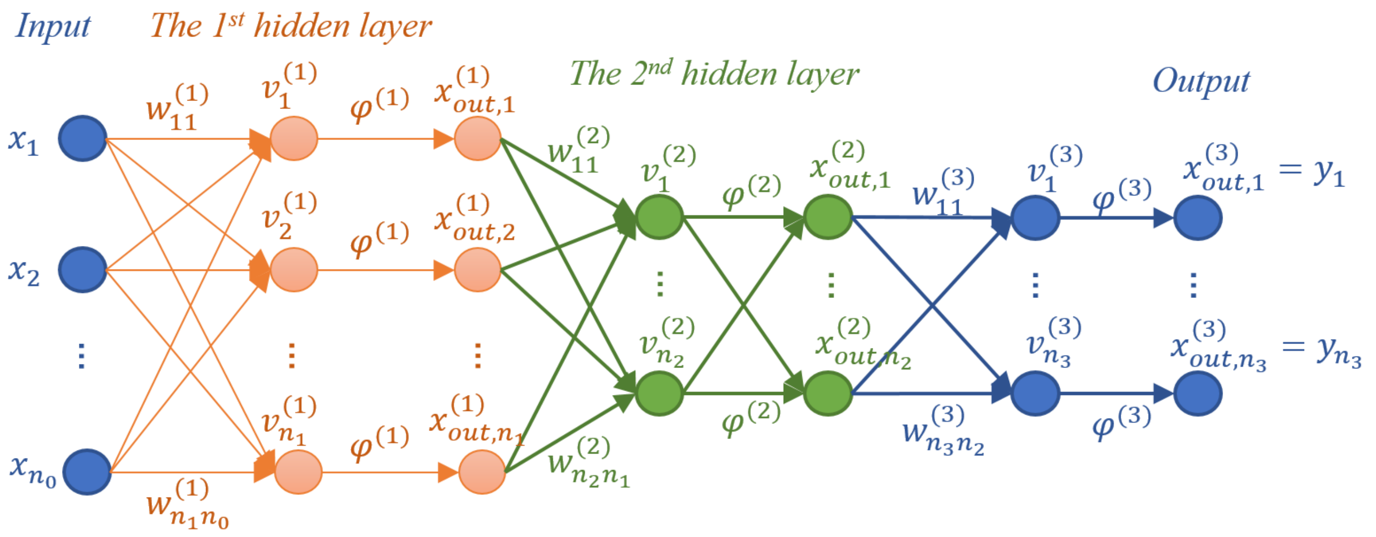

$$\begin{cases} w_{ji}^{(s)}(n+1) = w_{ji}^{(s)}(n) + \eta \delta_j^{(s)}(n) x_{\mathrm{out},i}^{(s-1)}(n) \\ \delta_j^{(s)}(n) = \left(d(n) - x_{\mathrm{out},j}^{(s)}(n)\right) \varphi^{(s)\prime}\left(v_j^{(s)}(n)\right) \text{ (output layer)} \\ \delta_j^{(s)}(n) = \left(\sum_{k=1}^{n_{s+1}} \delta_k^{(s+1)}(n) w_{kj}^{(s+1)}(n)\right) \varphi^{(s)\prime}\left(v_j^{(s)}(n)\right) \text{ (hidden layer)} \end{cases}$$

Support vector regression (SVR), Linear regression (LR)

Model setting

Fitting function for isotherms

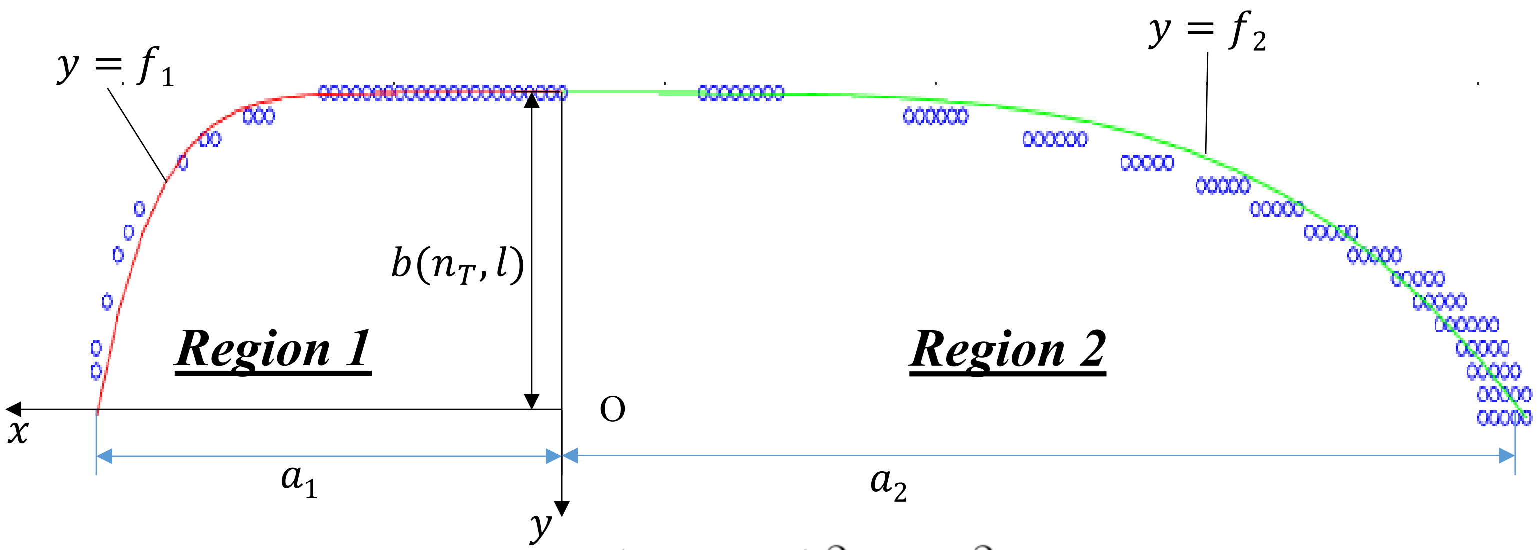

Ellipse function: $\frac{(x-x_f)^2}{a^2} + \frac{y^2}{b^2} = 1$

Polynomial function: $y = c_1 \left(x - x_f\right)^{index} + c_2$

Mean square errors: $\mathrm{MSE} = \frac{1}{n_s}\sum_{i=1}^{n_s}\left(Y_i - \hat{Y}_i\right)^2$

(Tested on No. 1~ No. 26)

Fitting performance

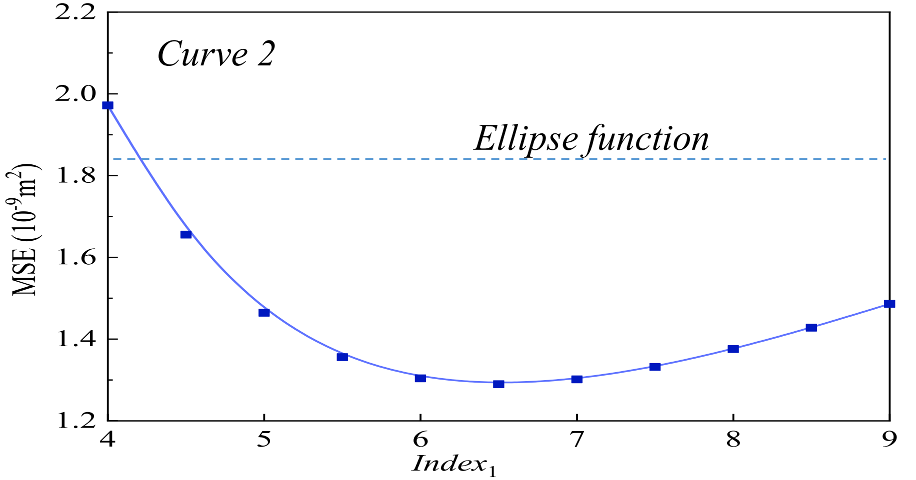

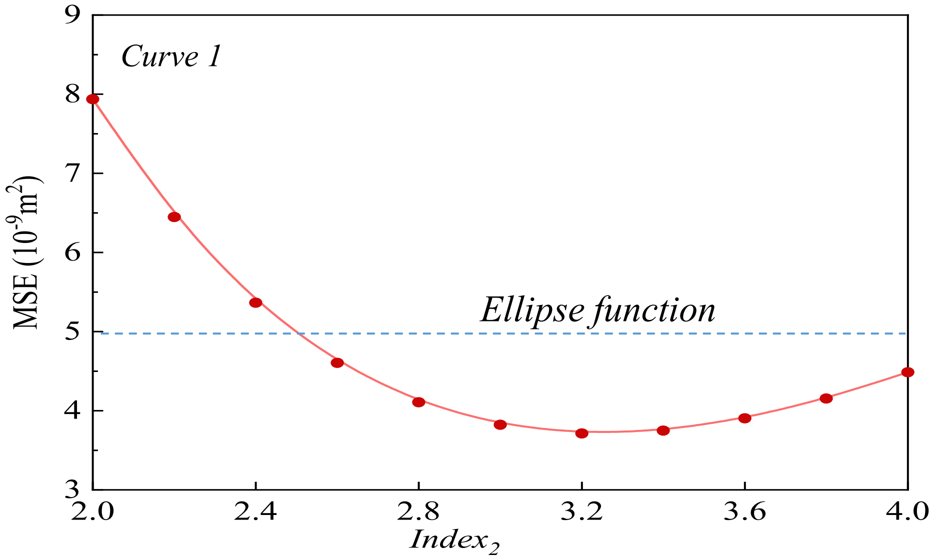

Model setting

Fitting performance of different functions

10th layer of sample no. 26

1000 K   1050 K   1110 K   1270 K   1340 K   1560 K

Region 1:

Ellipse fitting

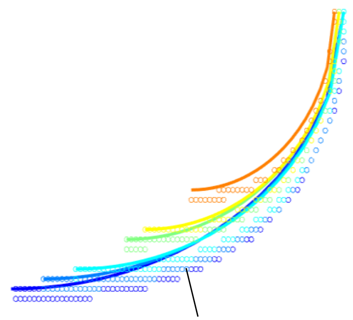

Isothermal points in thermal-fluid flow simulation

Polynomial fitting

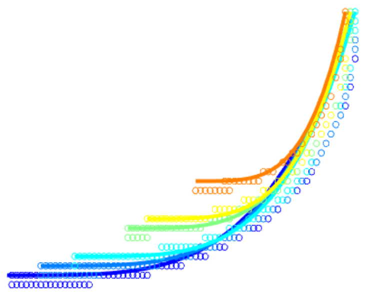

$Index_1 = 4$

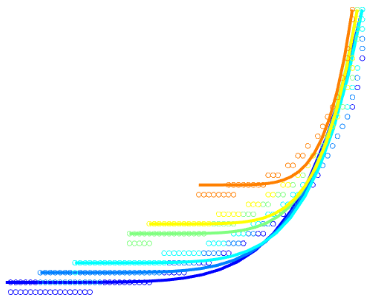

$Index_1 = 6$

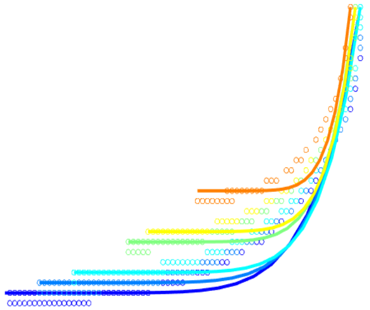

$Index_1 = 8$

Region 2:

Ellipse fitting

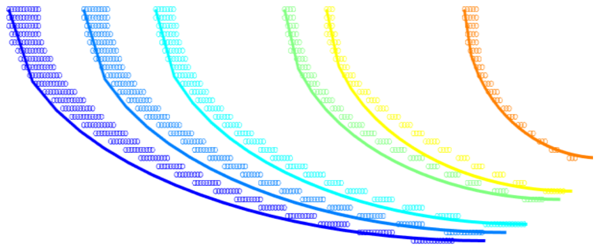

Polynomial fitting

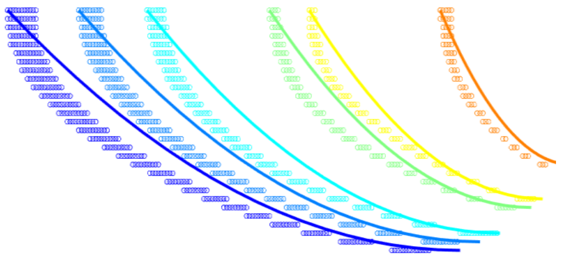

$Index_2 = 2$

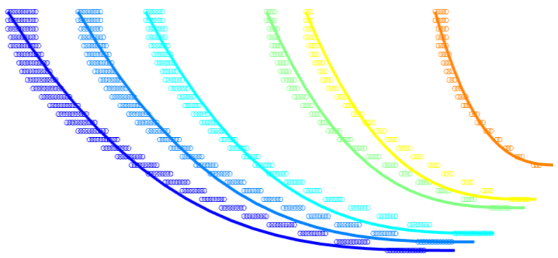

$Index_2 = 3$

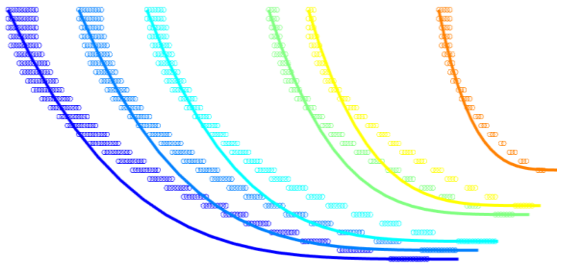

$Index_2 = 4$

Model setting

Training data sets: no.1~ no.26

Performance (MSE) of different algorithms on different output variables

Layer numbers ***L***

Algorithm	1000 K	1200 K	1400 K	1560 K
LR	10.04	7.96	8.04	7.77
QR	3.62	3.35	3.77	4.04
SVR	13.81	13.12	12.58	12.27
GPR	2.58	3.42	4.04	4.46

Slope angle ***θ***

Algorithm	1000 K	1200 K	1400 K	1560 K
LR	0.3218	0.3973	0.3577	0.2708
QR	0.2171	0.1822	0.1291	0.1110
SVR	0.3616	0.4267	0.3768	0.3018
GPR	0.1219	0.0432	0.0016	0.0096

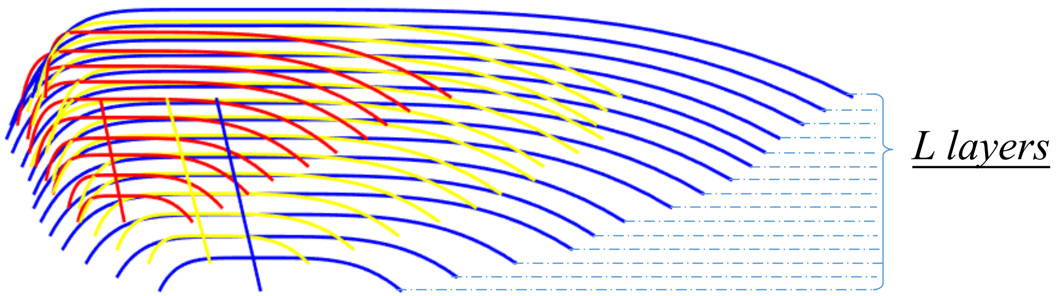

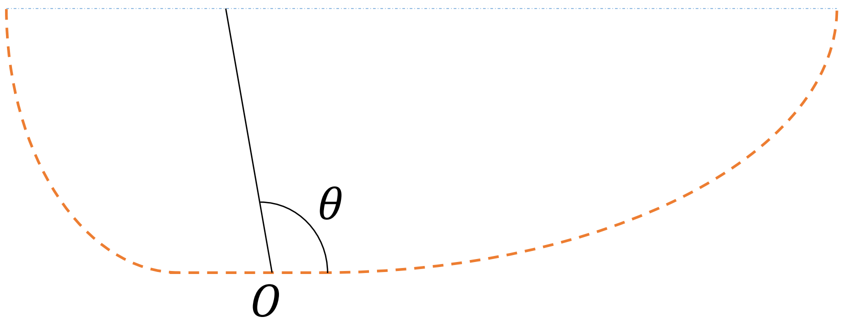

Model setting

Training data sets: no.1~ no.26

Performance (MSE) of different algorithms on different output variables

Relative distance Δx

Algorithm	1200 K	1400 K	1560 K
LR	2.79	8.20	6.59
QR	2.03	5.75	4.84
SVR	3.11	10.82	8.13
GPR	5.87	14.83	8.65

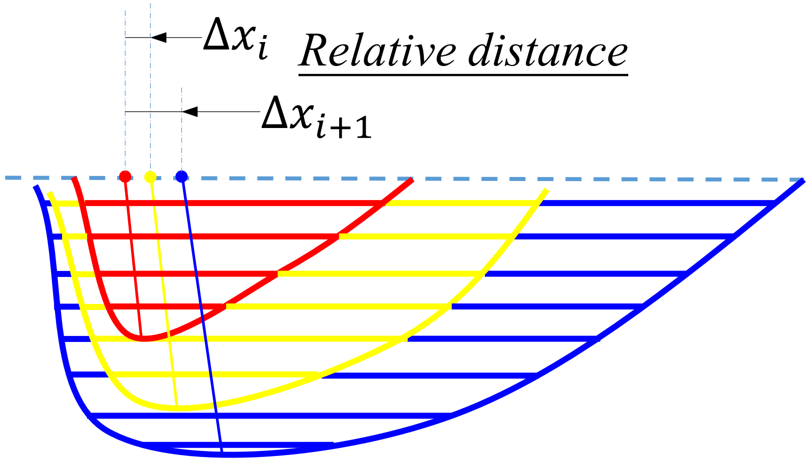

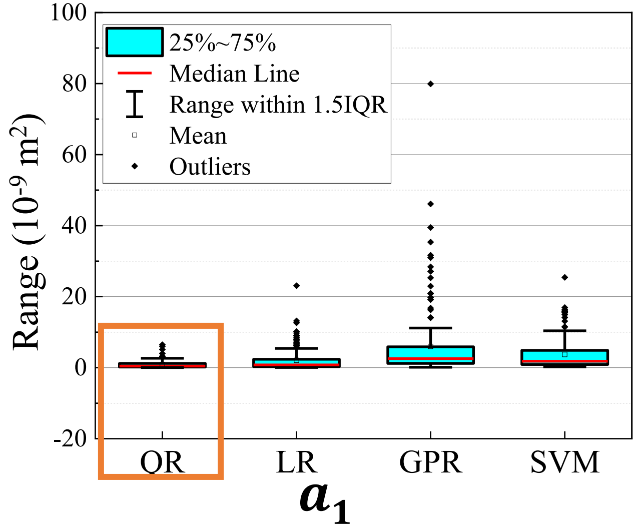

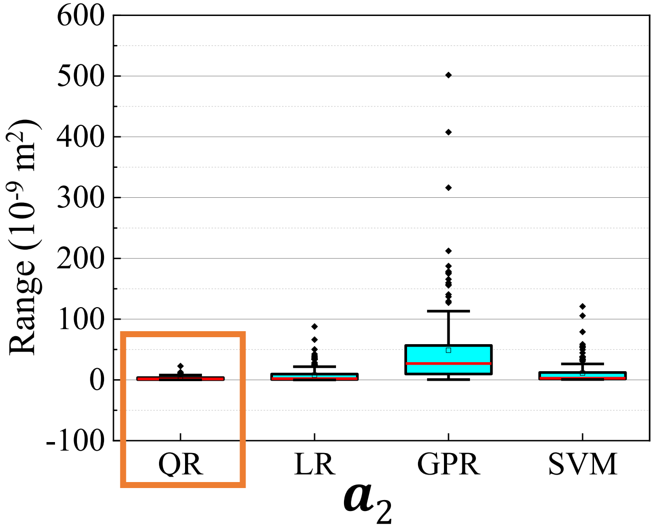

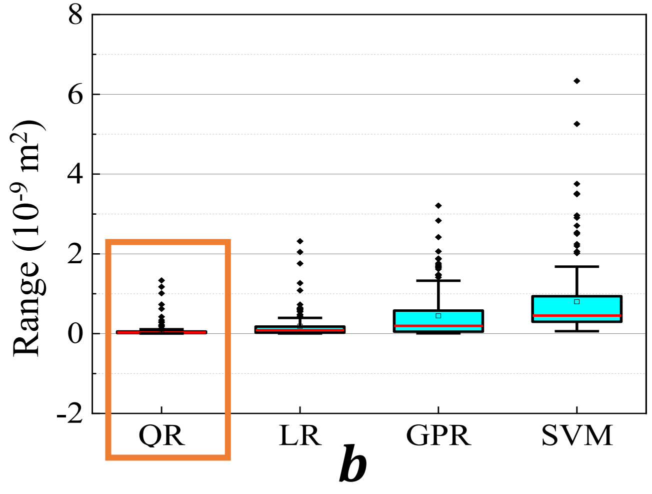

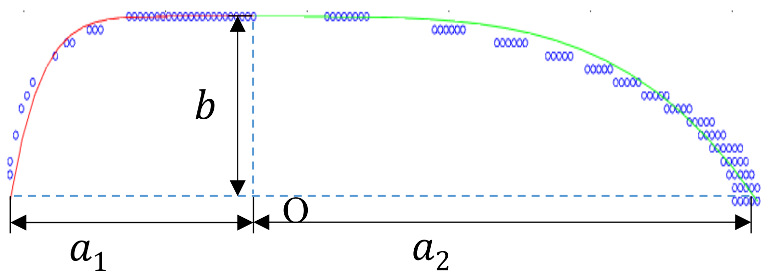

Model setting

Different training datasets

Testing Sample no. 41
V =1 m/s
P =40 W

Predicted isotherms of Region 2

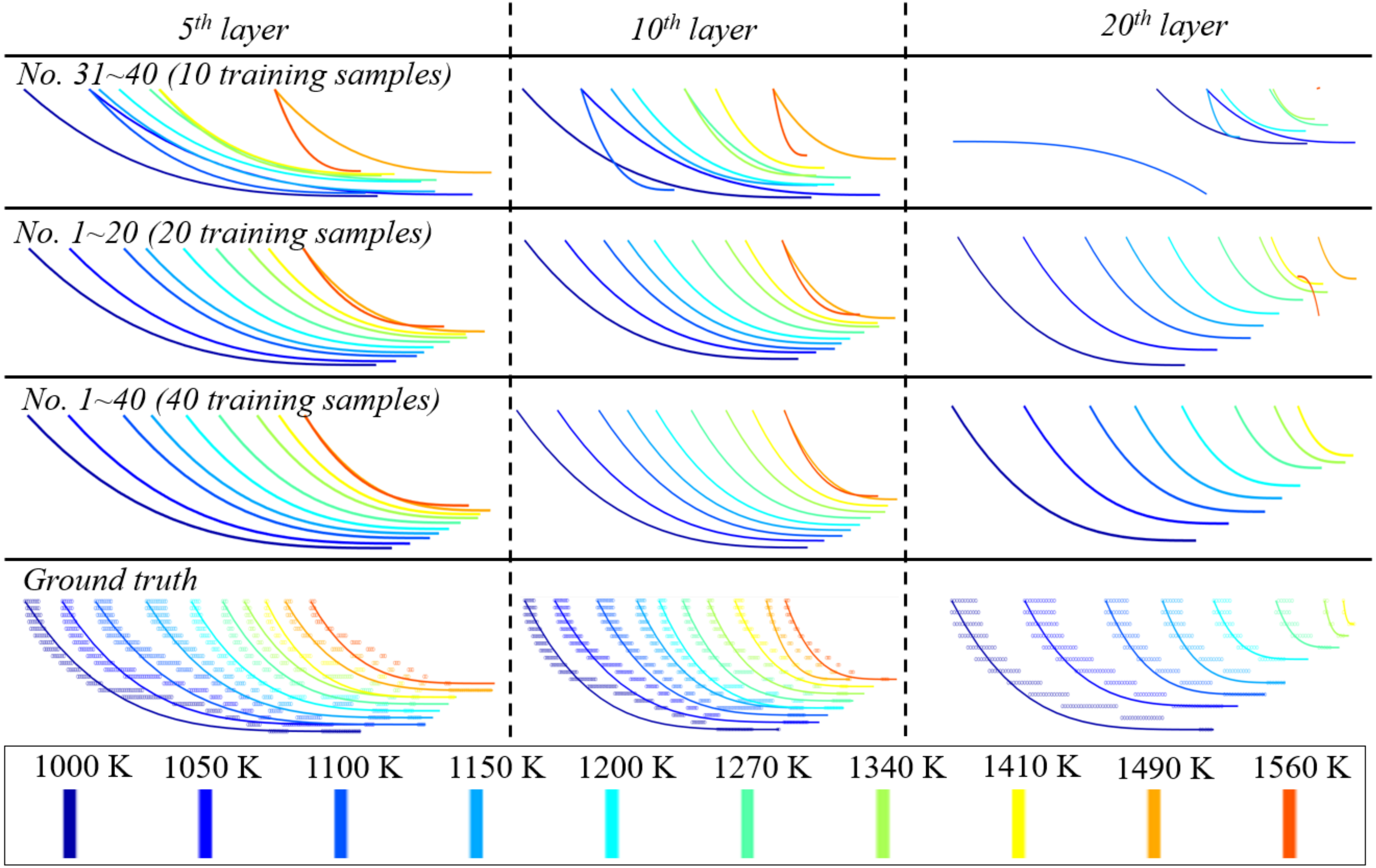

Model evaluation

Temperature field reconstruction

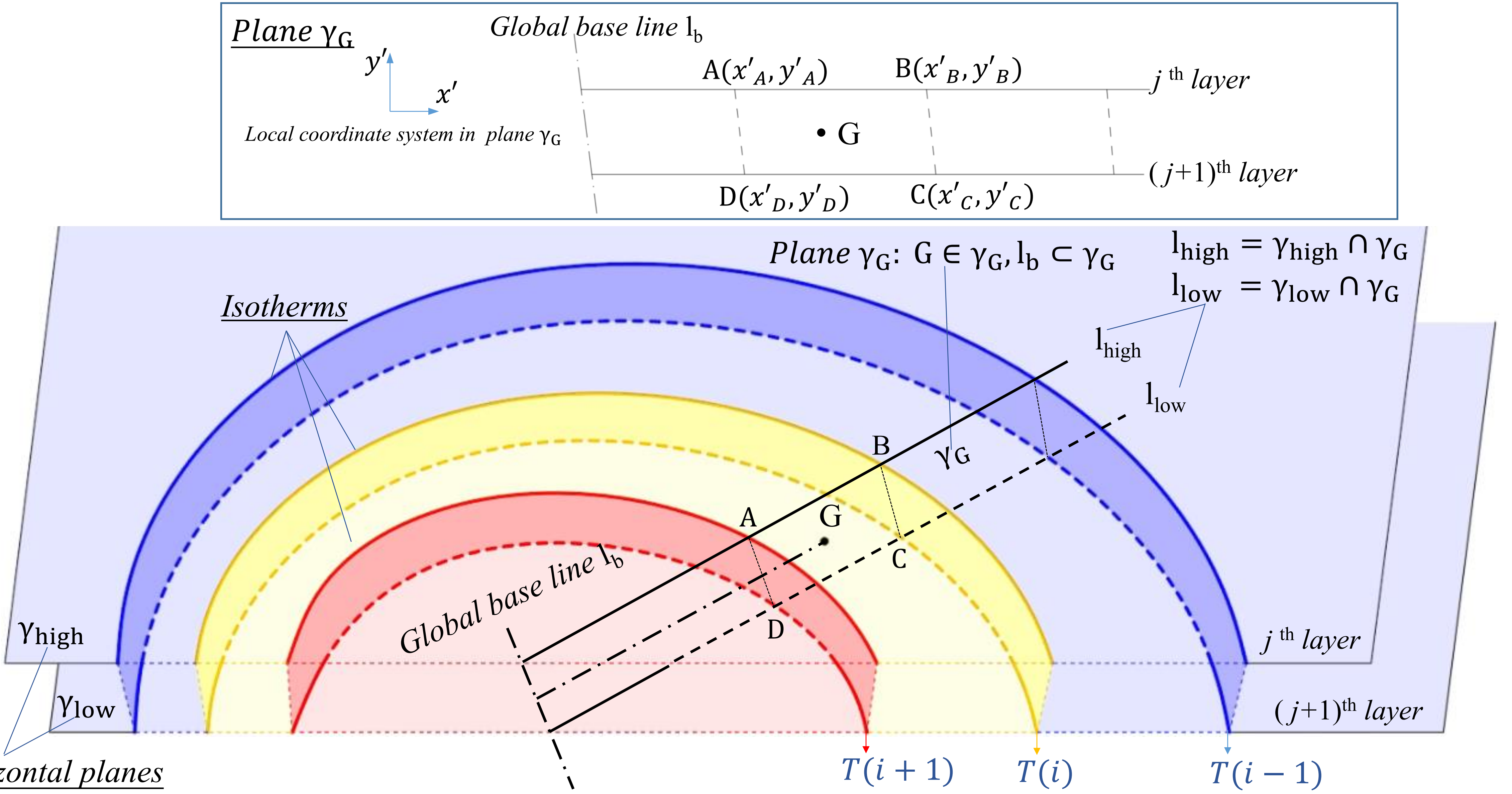

Model evaluation

Training: No. 1~40
Testing Sample: no. 41, V =1 m/s, P =40 W

MMLDT CSET 2021

NUS National University of Singapore

Temperature history (Inconel 625)

Predicted results

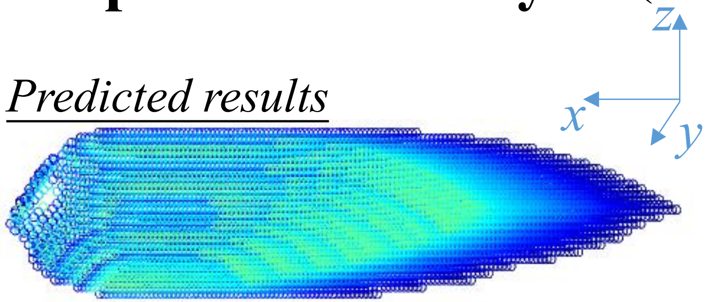

CFD results

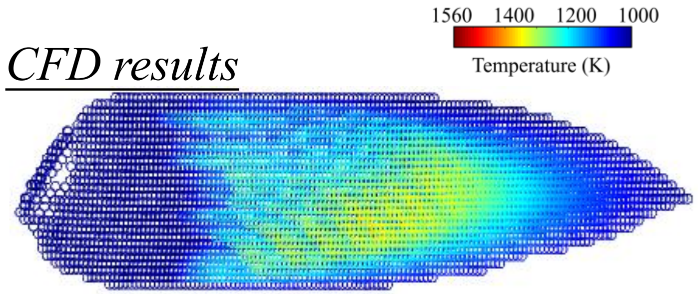

Temperature difference

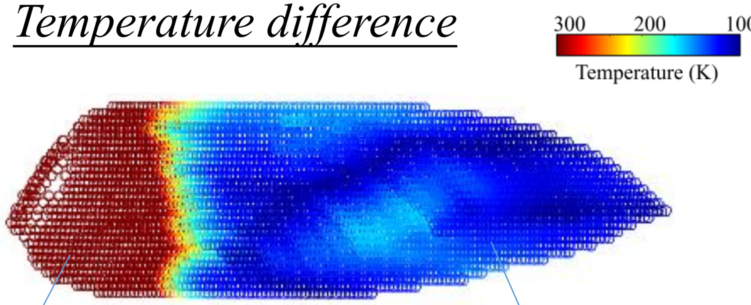

Over-prediction of the molten pool half-length a_1

($Index_1$, $Index_2$) for the isotherms: (5, 4) & (6, 3)

O and Q: *At the molten pool boundary*

P: *Inside the molten pool*

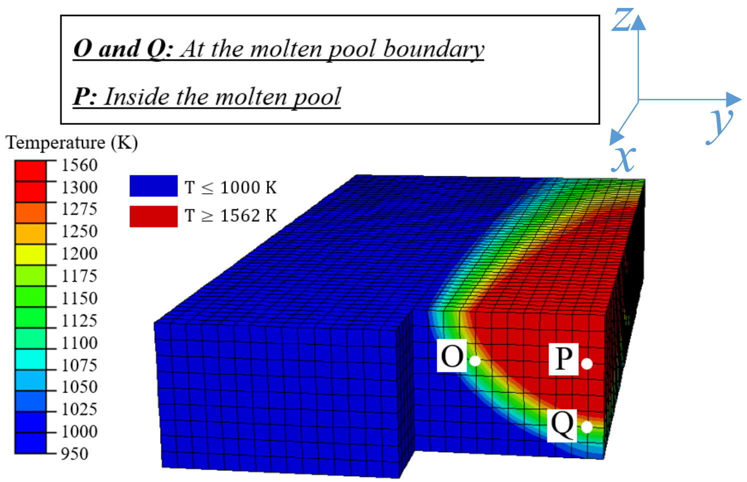

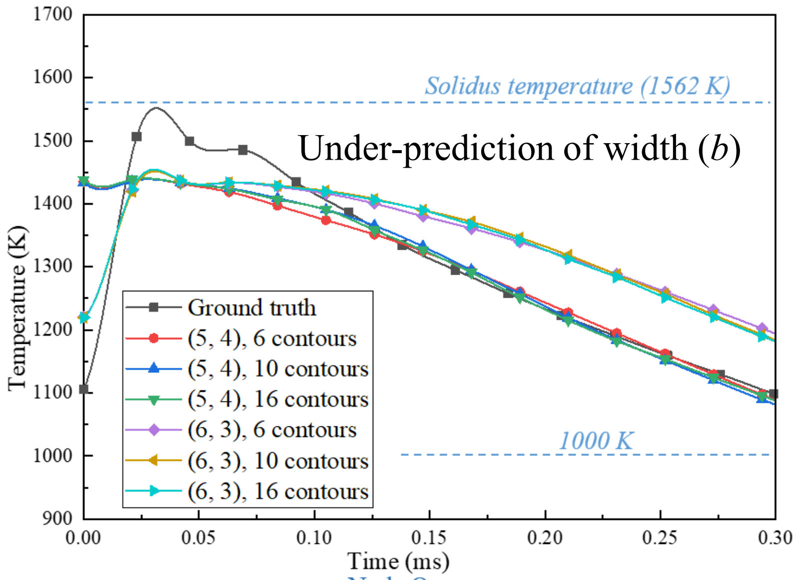

Node O

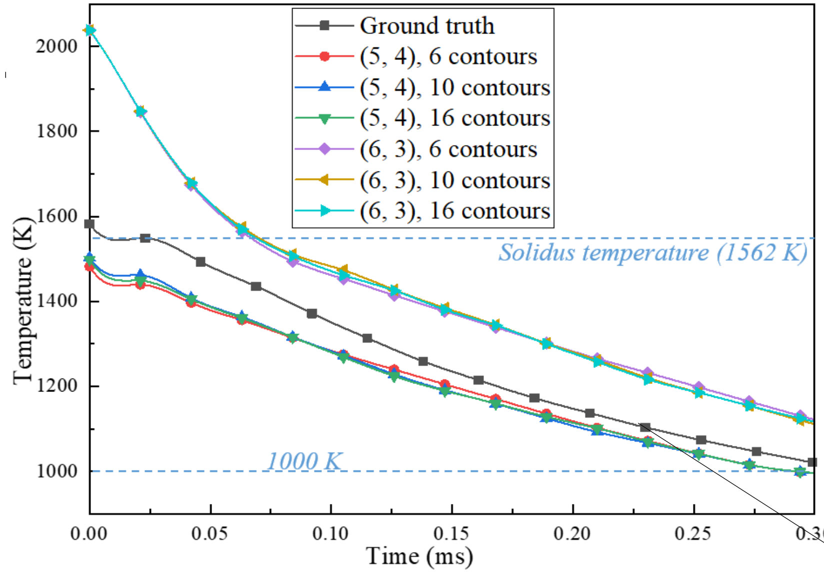

Node P

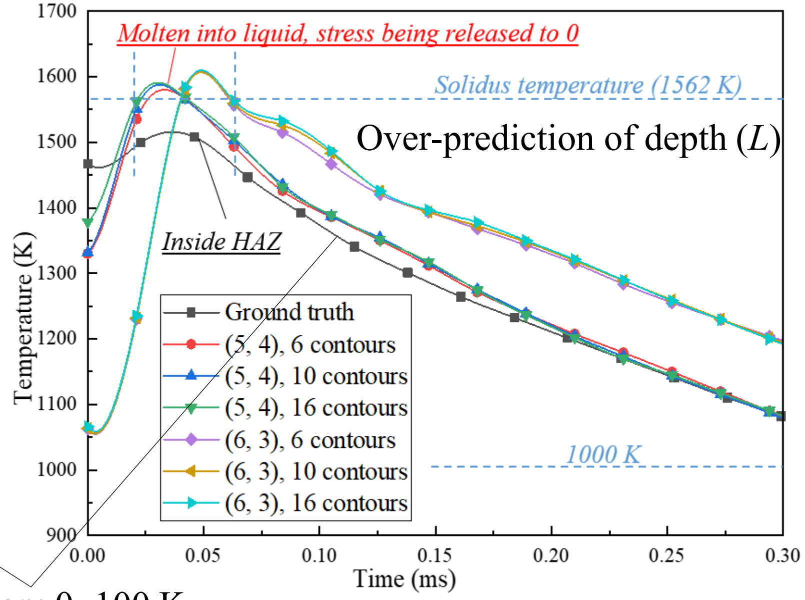

Node Q

Deviation: 0~100 K

Model evaluation

Thermal stress history on node P

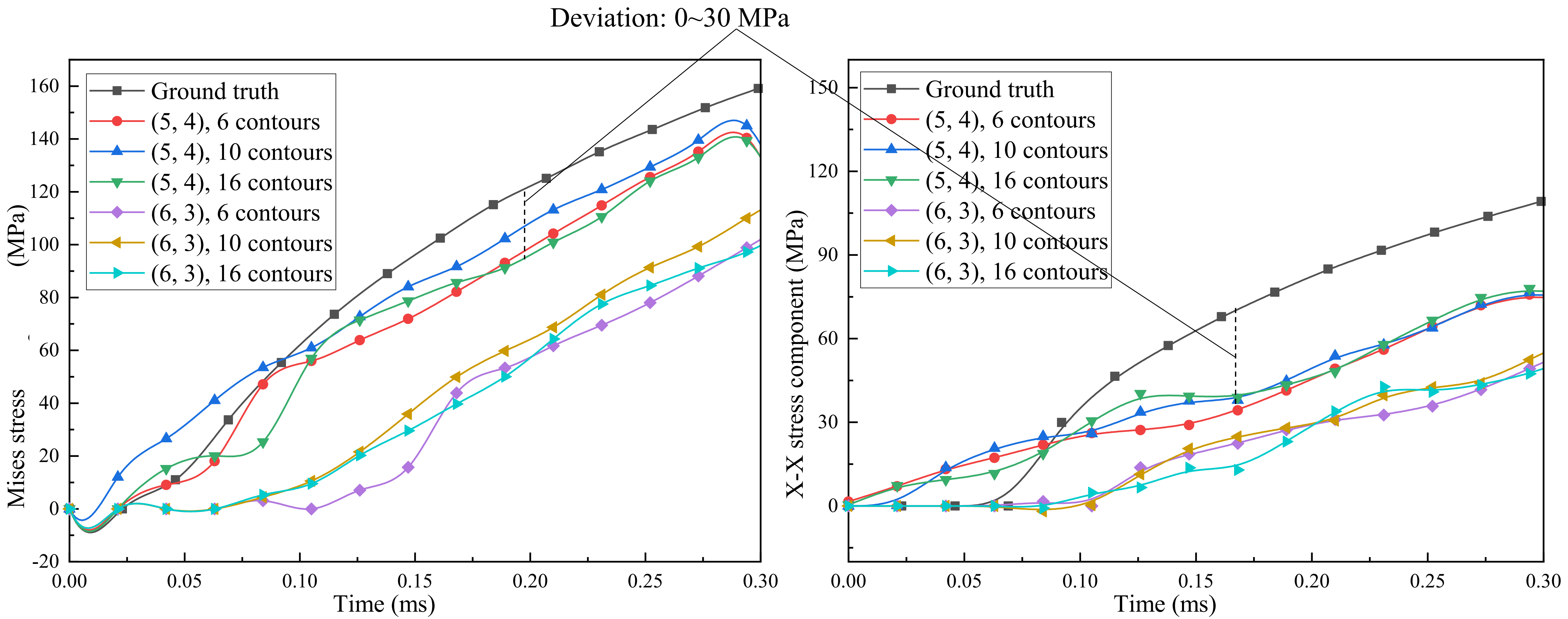

(Similar trend and level)

Model evaluation

Thermal stress history on node P

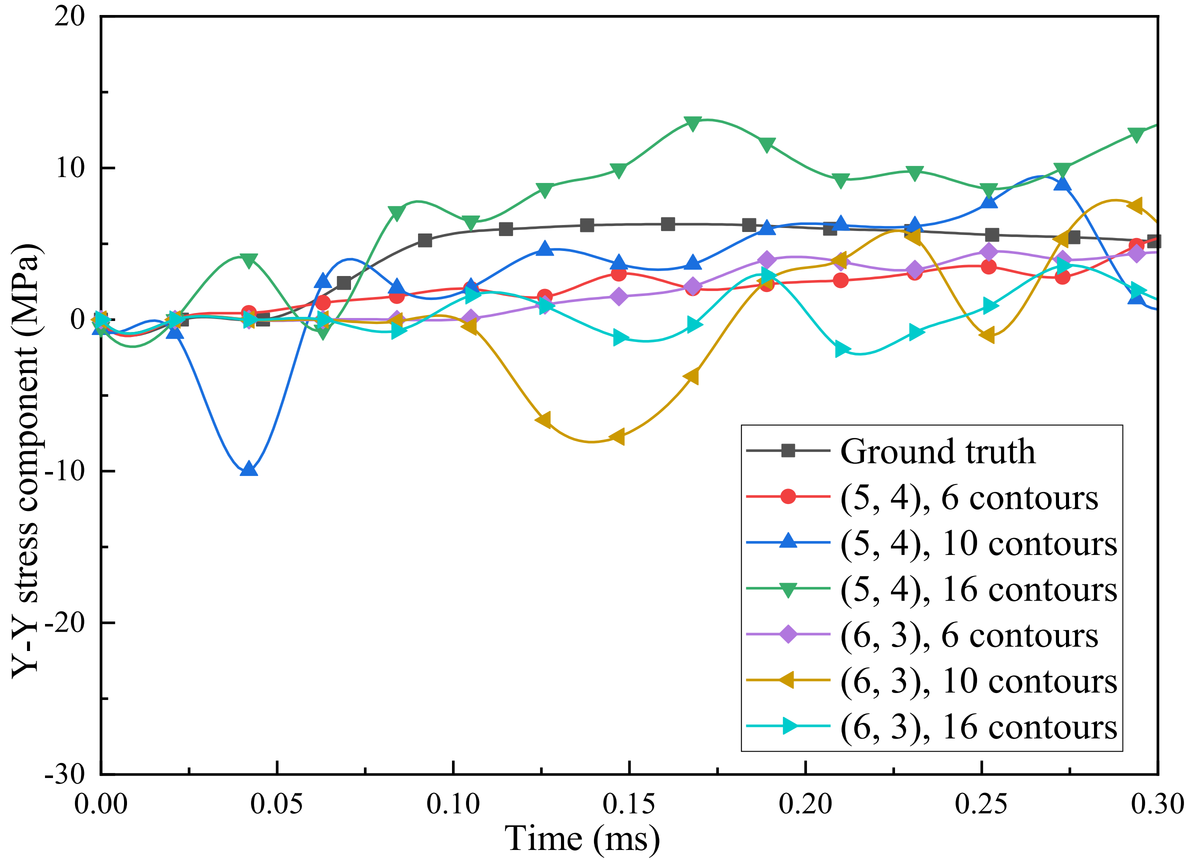

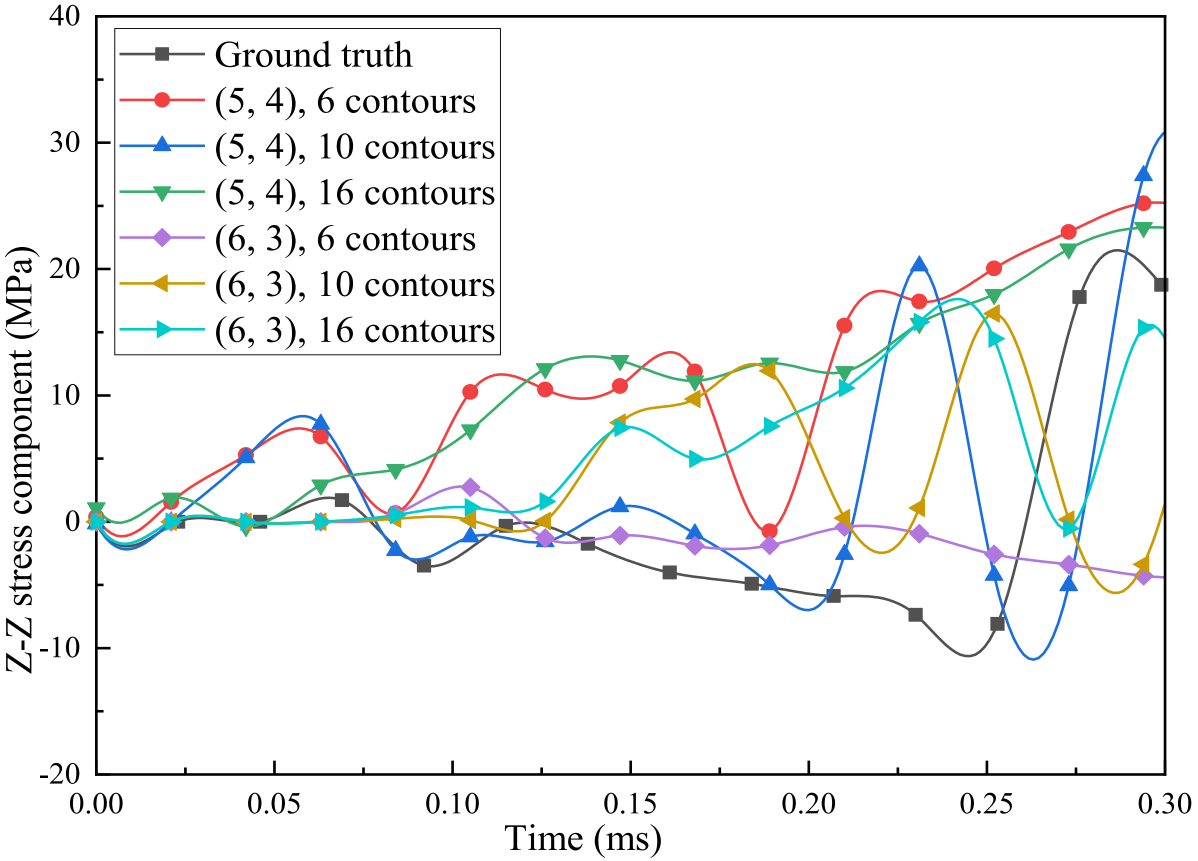

Due to the small level of the Y-Y and Z-Z stress components, the deviations affect less on the Mises-stress.

Model evaluation

Training: No. 1~40
Testing Sample no. 42, V =1 m/s, P =85 W

MMLDT CSET 2021

NUS National University of Singapore

Grain growth

Average grain volume:
Data-driven prediction: 1032.2μm3
Ground truth: 1285.5μm3.
Deviation: 19.7 %

Ground truth

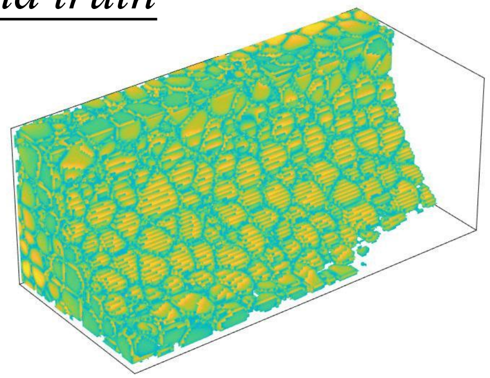

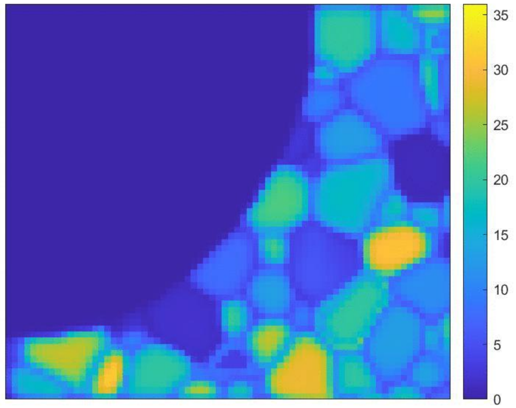

Prediction

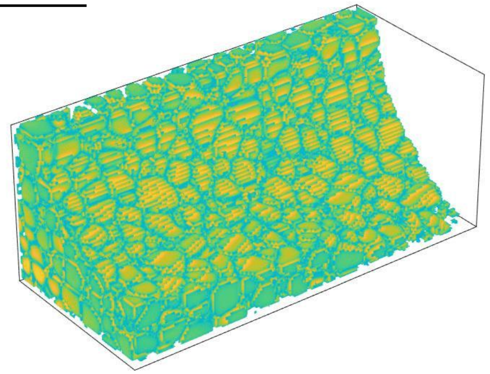

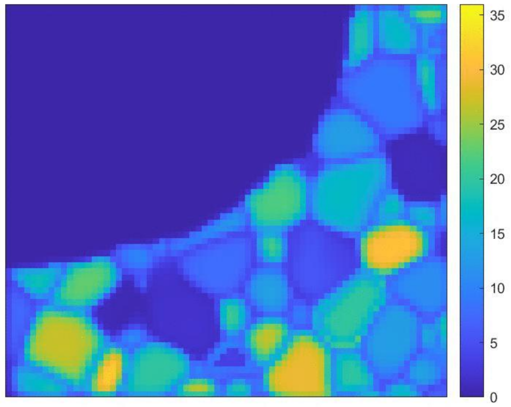

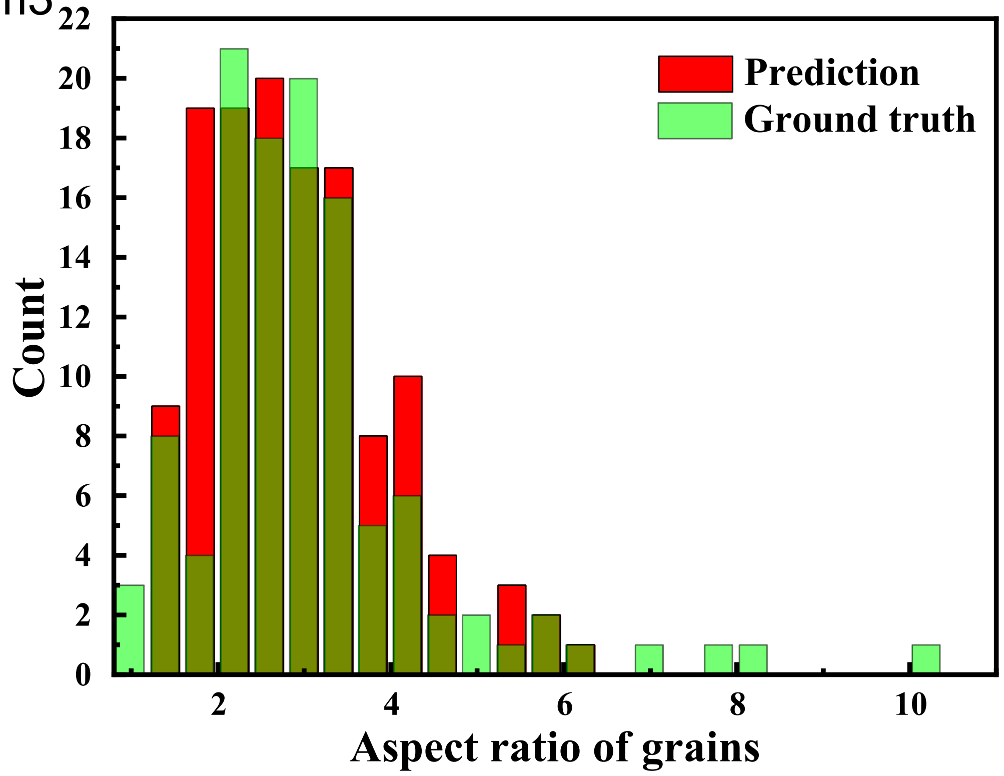

Less grains with high aspect ratios in the prediction due to the under prediction of the molten pool depth.

Computational cost

The computational cost of the data-driven predicted model is reduced by at least 70 %.

	Node number	CFD data	Data-driven prediction
Case 1	21620 (12 CPUs)	70 min	20 min
Case 2	168636 (24 CPUs)	11h 15 min	2 h 14 min

Application: Data-driven predicted 5-track 3-layer AM case

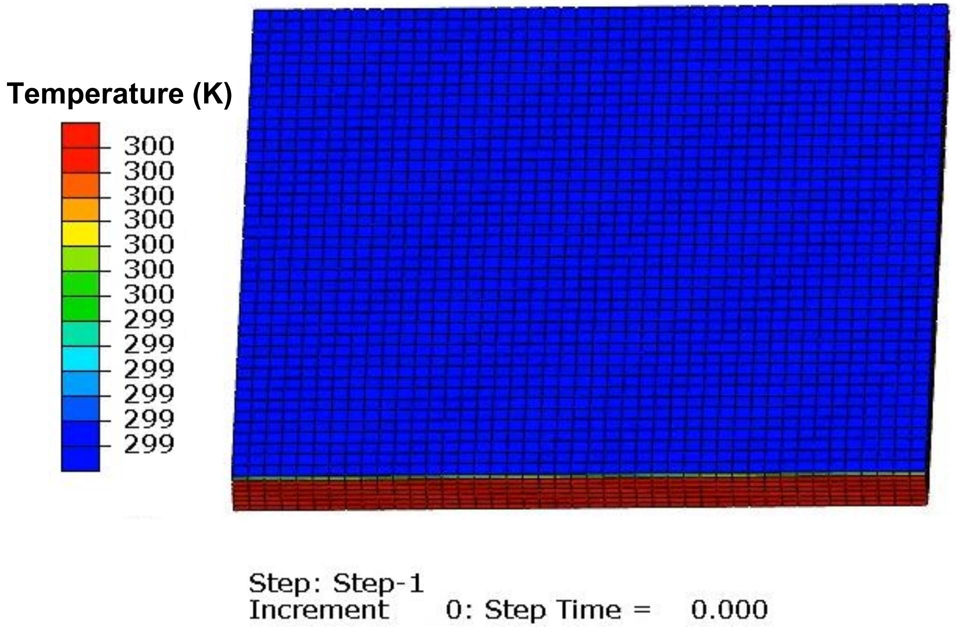

- **No heat transfer**
- **No thermal-fluid flow calculation**
- **No CFD temperature files loading**

The simulation case with 1400+ steps can be finished within 36 CPU hours, which is nearly impossible for other thermo-mechanical models.

Thank you

Fan Chen

Email: e0348805@u.nus.edu

Yan group website: https://blog.nus.edu.sg/yanwt/

Fan Chen, Min Yang, Wentao Yan*, Data-driven prognostic model for temperature field in additive manufacturing based on the high-fidelity thermal-fluid flow simulation. (under review)